The Effect of Segregation on the Formation of Austempered Ductile Iron

J. M. SCHISSLER and J. SAVERNA

Alloy segregation at the solidification cell boundaries can have a very important influence upon the kinetics of the bainite reaction. The two stages usually observed in a homogeneous matrix after isothermal holding in the range of temperatures 350 to 450 °C can be described as follows: 1 — $\gamma \rightarrow (\alpha) + (\gamma)$; 2 — $(\alpha) + (\gamma) \rightarrow \alpha +$ silicocarbides. These reactions are functions of the elements in solution in the matrix. For this reason, segregated elements affect very sensitively the evolution of the two basic reactions. The solidification cell boundaries are often not completely transformed to bainite, which explains the presence of martensite observed in these areas. The influence of the size of the solidification cells has also been studied. The austenitization conditions are also very important. At the opposite extreme, the bainitic reaction of the matrix located along the graphite interface evolves more quickly than that observed in the matrix or at the cell boundaries.

INTRODUCTION

This study discusses reactions in unalloyed ductile iron. This basic presentation is necessary for the understanding of the complexity caused by nonuniformity of the repartition in the matrix of various alloying elements such as nickel, molybdenum, and copper.

In fact, even in a usual so-called "unalloyed ductile iron" a segregation of residual content of manganese can be observed and the structure of austempered ductile iron is rather complex.[1-5]

For this reason this report will be presented in two parts: (1) the bainite reaction in a homogeneous matrix and (2) application to austempered ductile iron.

THE BAINITE REACTION IN SILICON STEELS

Figure 1 represents the TTT curves of the homogeneous matrixes of two wrought steels.[6,7] Figure 1(a) shows a steel without silicon and Figure 1(b) a steel with 3.7 pct silicon. Compared to the unalloyed steel, the silicon steel requires a higher temperature for complete austenitization, and the incubation time of pearlite and the bainite formation is increased. That means that the silicon alloyed steel has better hardenability. We can also observe some separation between the temperature ranges of the pearlite and the bainite reaction. Silicon does not affect the M_s temperature very much but raises the Al temperature.

In a hypereutectoid silicon alloyed steel, the TTT curve shows several important points (Figures 2(a) and (b)):

1. Bs temperature: the bainite start temperature. For this kind of alloy, Bs is usually at about 450 °C.
2. The bainite formation which occurs between the Bs and the M_s temperatures presents a characteristic feature. At 350 °C the reaction is incomplete. Figure 2(a) indicates that the bainite reaction goes to completion above and below the temperature ranging from 320 to 370 °C.
3. Depending upon the temperatures at which the product is obtained, the bainite formation is usually divided in two groups: (a) one situated between the temperature Bs and

J. M. SCHISSLER and J. SAVERNA are with Laboratoire de Métallurgie associé au CNRS U.A. 159, Ecole des Mines Parc de Saurupt, 54042 Nancy Cedex, France.

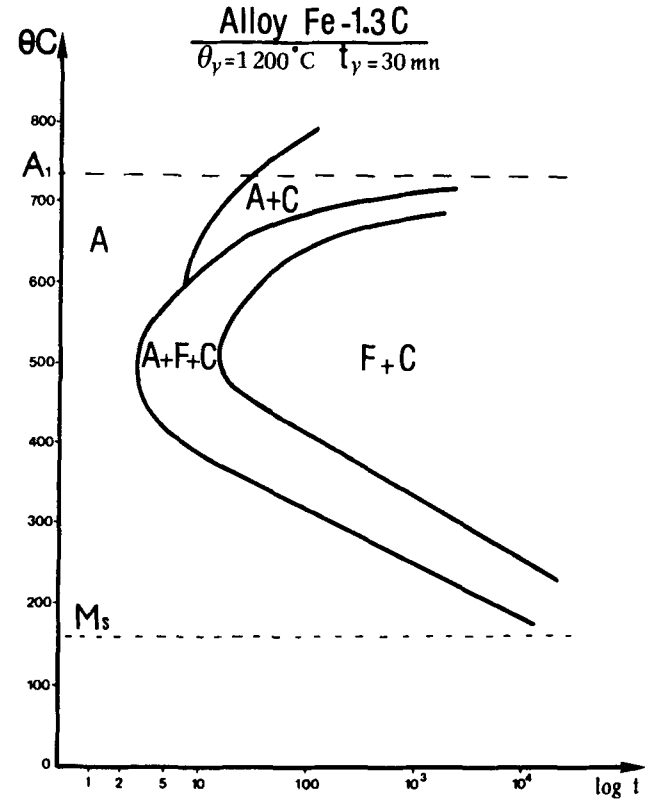

(a)

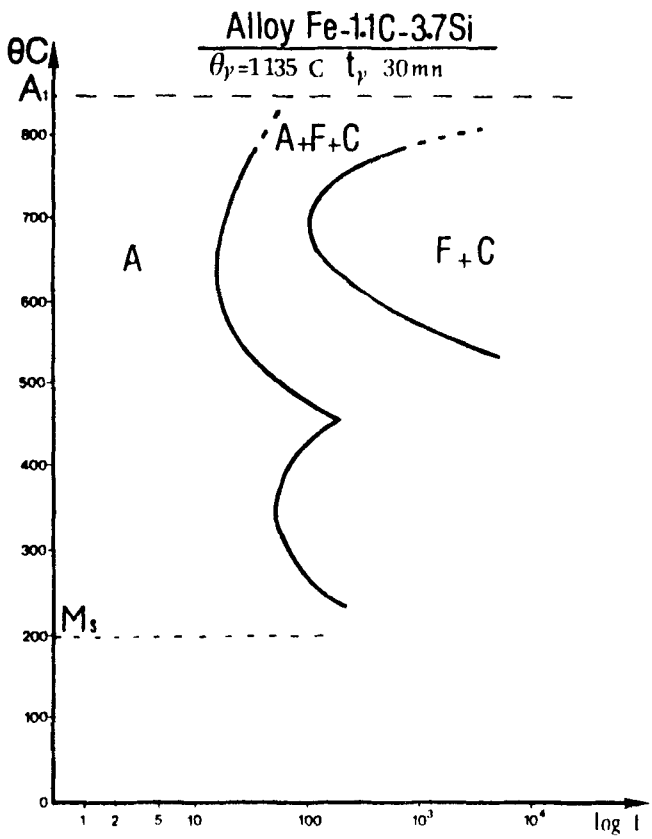

(b)

Fig. 1—(*a*) TTT curve of the homogeneous matrix of a wrought Fe-C steel. (*b*) TTT curve of the homogeneous matrix of a wrought Fe-C-Si steel.

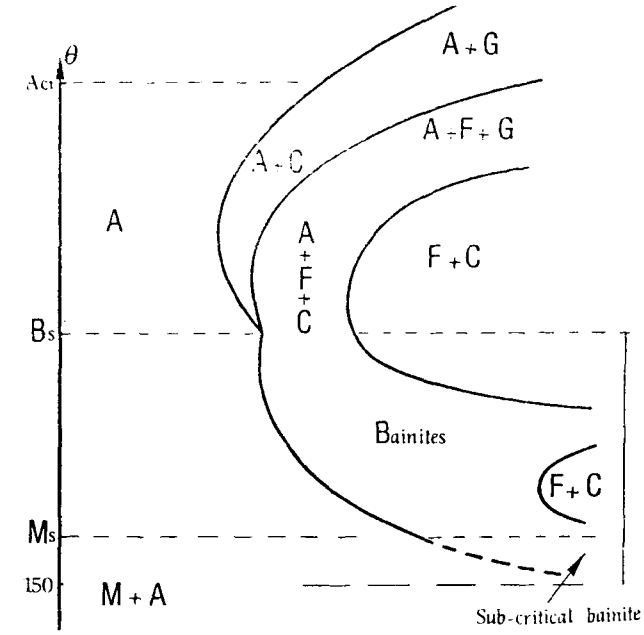

(a)

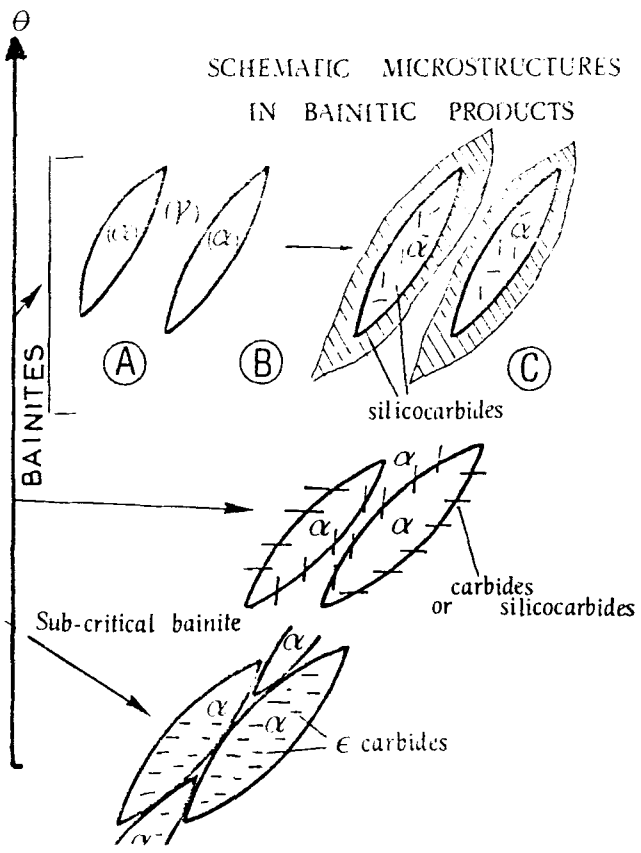

(b)

Fig. 2—(*a*) Schematic TTT curve of a hypereutectoid Fe-C-Si homogeneous matrix. (*b*) Schematic microstructures in bainitic products.

350 °C called "upper bainite"[7] and (b) the other, located between 350 °C and the M_s temperature, called "lower bainite".[8]

Sometimes there is also another bainite called "subcritical bainite" formed between the M_s temperature and 150 °C, but

it is possible to observe this only after long isothermal holding times in steels having an M_s temperature above 150 °C.[9]

The upper bainite reaction can be separated into two stages. In silicon-containing alloys silicon is a very strong inhibitor of carbide formation.[2,7] These two stages can be described by the following:

(1) The austenite is transformed in an aggregate of two phases: ferrite and austenite. The new formed ferrite is supersaturated in carbon and the remaining austenite is enriched in carbon. This new enriched austenite is also called "post bainitic austenite".

(2) These two phases are decomposed into ferrite and silicocarbides by an *in situ* transformation of the supersaturated austenite and an aging of the supersaturated ferrite. The carbides will be different if they originate inside the austenite or inside the ferrite. Most of these new carbides are situated along ferrite boundaries and the rest inside the ferrite. At temperatures below 350 °C, and at the end of the reaction, the carbides are precipitated across the interface between ferrite and austenite, and carbides belong to the silicocarbides family. At lower temperatures, the lower bainite is composed of ferrite with a very fine dispersion of ε carbides oriented inside the ferrite.

In a 4 pct silicon 1 pct carbon steel transformed at 400 °C, at the end of the first stage a typical X-ray diffractogram is shown in Figure 3. From the location of the lines one can calculate the carbon content of the austenite. In this case the post bainitic austenite contains 2 pct carbon and the M_s temperature falls from +200 °C to −130 °C. This is the result of both the strong carbon enrichment of this new austenite and the action of strains. Observed by optical microscopy, the typical structure of the bainite obtained at the end of the first stage is typical and is shown in Figure 4. In this case, the structure contains 50 pct post bainitic austenite.[7] Observed by electron microscopy on thin foils (T.E.M. observation), the ferrite is composed of very small elongated cells (Figure 5). A fundamental study of the mechanism indicates that this first stage of the bainitic product is obtained by the combination, in order, of a shear mechanism like a martensitic transformation, followed by a diffusion of carbon toward the surrounding austenite in order to enrich it.[7] In Figure 6, one can see that the austenite is free of martensite.

The morphology observed by optical microscopy at the end of the second stage shows the evolution of the structure (Figure 7). T.E.M. observation permits the study of the *in situ* decomposition of the enriched austenite and the aging of the ferrite. The precipitates are silicocarbides (Figures 8(a) and 8(b)).[7] Inside the ferrite (Figure 9(a)) or along the ferrite (Figure 9(b)) the morphology of these silicocarbides is different. This is a consequence of the kind of reactions which occurred in the phases.

The observations of lower bainite formed at 330 °C (Figure 10(a)) or at 300 °C, (Figure 10(b)) indicate the evolution of the morphologies which are present in the bainitic products.[10,11] For example, in the same steel, lower bainite (Figure 11(a)) appears very different from high carbon martensite tempered at 200 °C (Figure 11(b)).[9]

The TTT curve of a homogeneous matrix can be explained by the coexistence of these two reactions (Figure 12). The times necessary to accomplish these reactions

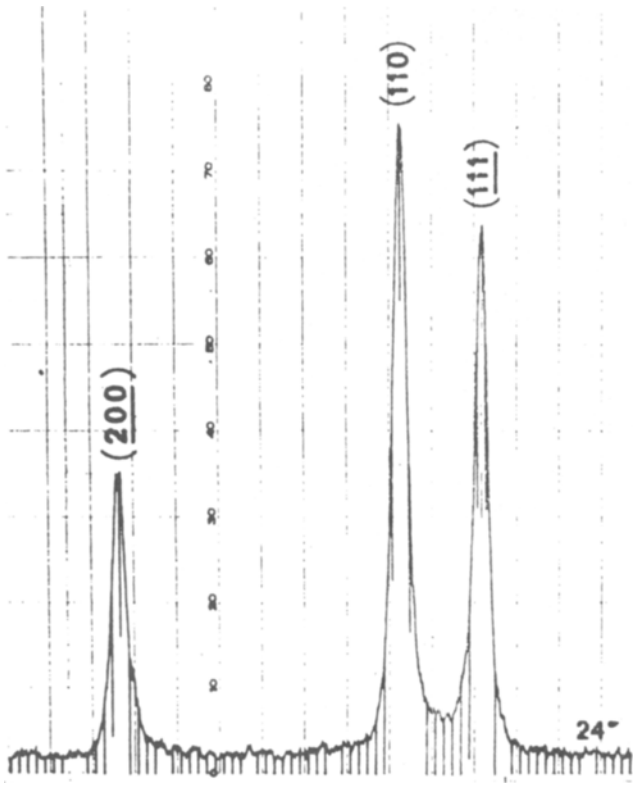

Fig. 3 — X-ray diffractogram (K_α Co) of the matrix at the end of the first stage (Fe-C-Si steel).

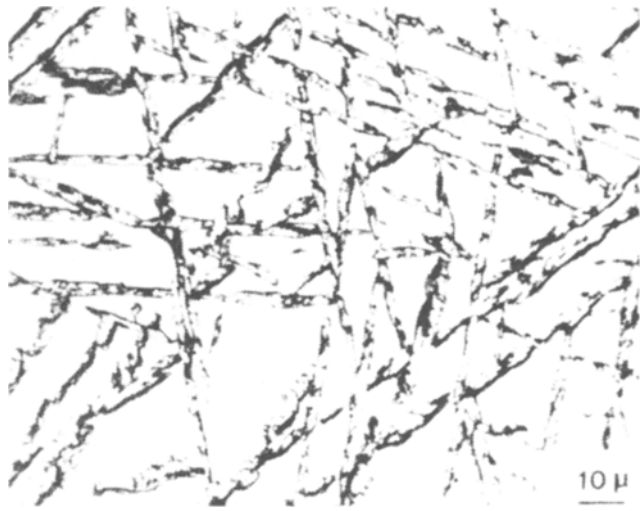

Fig. 4 — Optical microscopy (OM) observation of the matrix at the end of the first stage (F-C-Si steel).

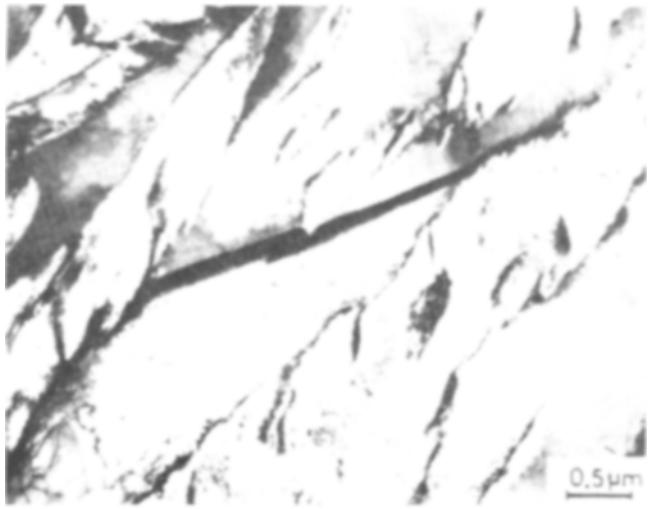

Fig. 5 — TEM observation of the matrix at the end of the first stage.

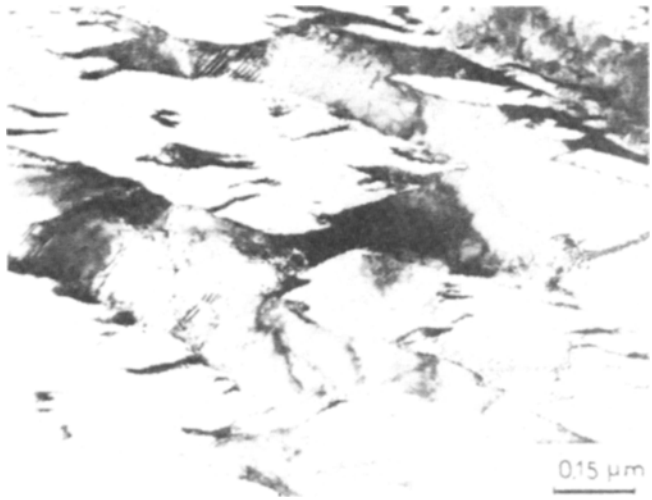

Fig. 6 — TEM observation of the small elongated ferritic cells.

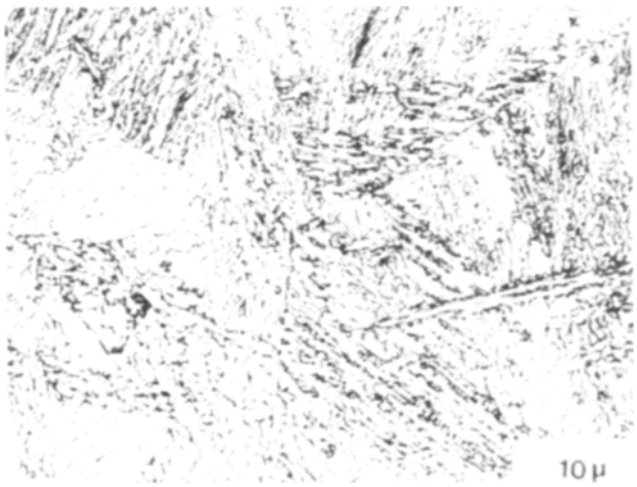

Fig. 7 — OM observation of the matrix when the second stage is achieved (Fe-C-Si steel).

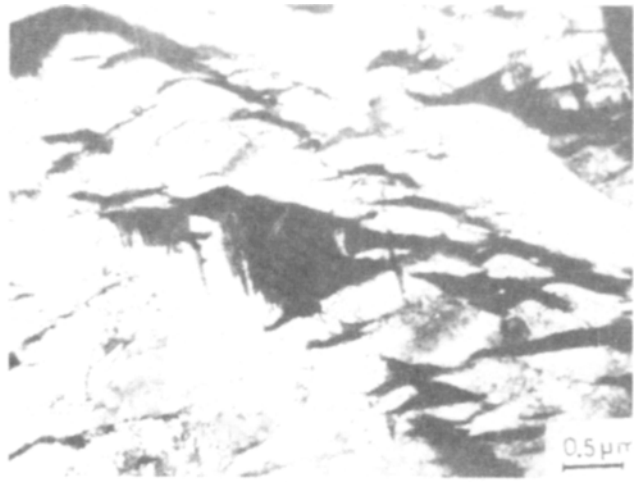

(*a*)

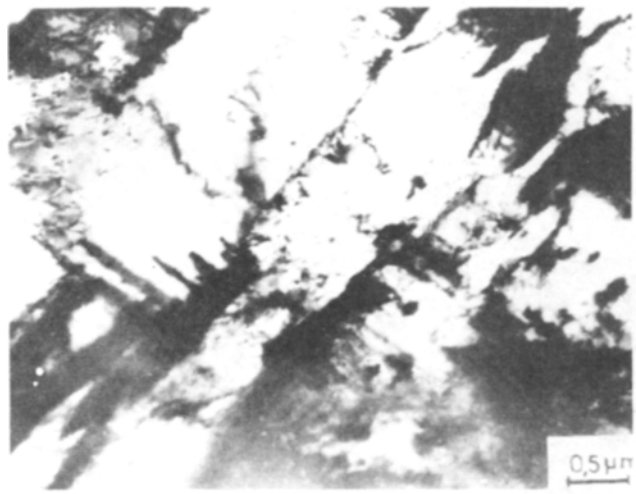

(*b*)

Fig. 8 — (*a*) TEM observation of the carbide precipitation which has occurred at the former (α)-(γ) interface (Fe-C-Si steel). (*b*) TEM observation of the aging of the supersaturated ferrite of the first stage.

are a function of the temperature of the reaction and the level and nature of the alloying elements. The incubation times for the reactions are functions of the same factors. At 350 °C the second stage is very difficult to obtain.

The influence of the carbon level of the high temperature austenite, the parent phase, on the duration of the first stage at 400 °C is very important (Figure 13). The higher the carbon level, the more time is necessary to complete the first stage. This carbon level is also a function of the austenitization temperature and time and the silicon level of the austenite. For the same austenitization conditions the carbon content becomes less important as the silicon content is increased (Figure 14).[12]

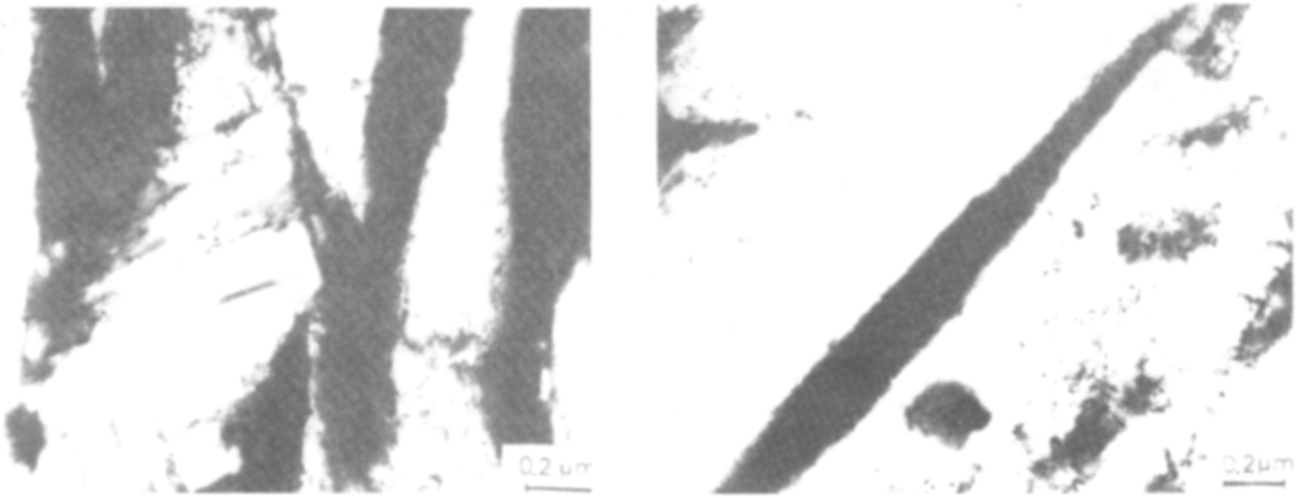

(a) (b)

Fig. 9—(*a*) Same area of Fig. 8(b) but at higher magnification. (*b*) TEM observation of the silicocarbide along the ferritic cells when the second stage is well achieved.

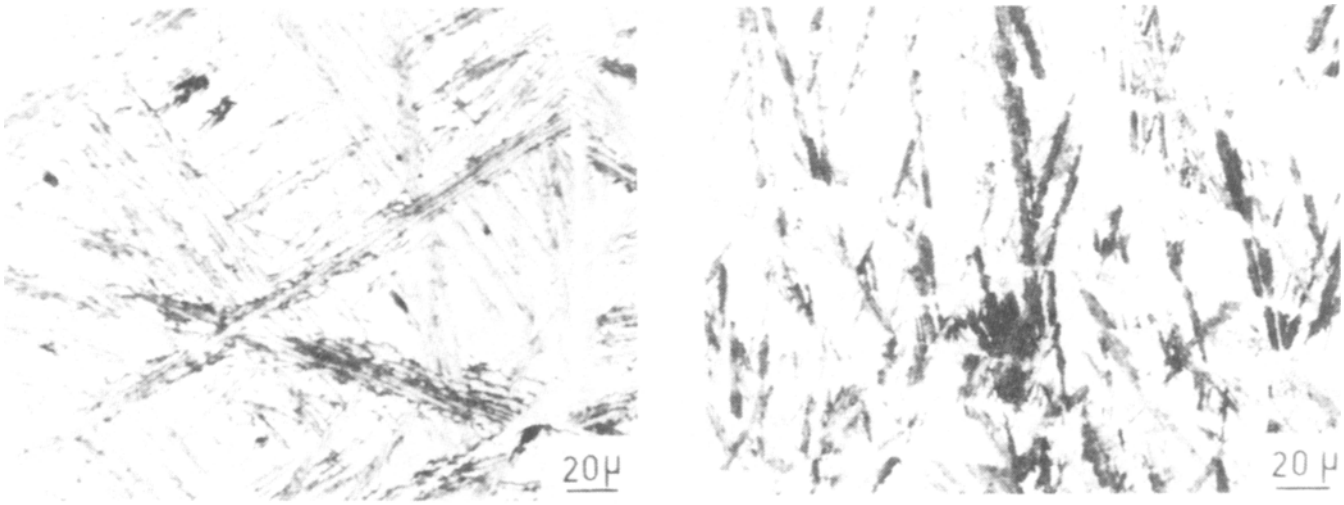

(a) (b)

Fig. 10—(*a*) OM observation of lower bainite formed at 330 °C. (*b*) OM observation of lower bainite formed at 300 °C.

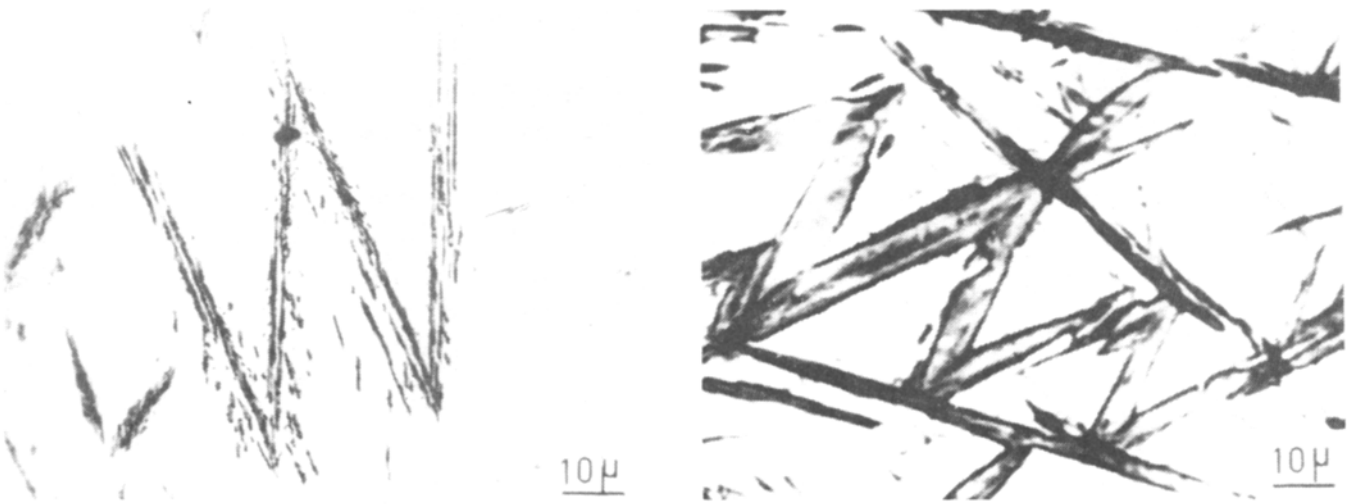

(a) (b)

Fig. 11—(*a*) OM observation of lower bainite occurring at temperatures just above the M_s temperature of the Fe-C-Si steel. (*b*) OM observation of a 200 °C tempered martensite (same steel as for (a)).

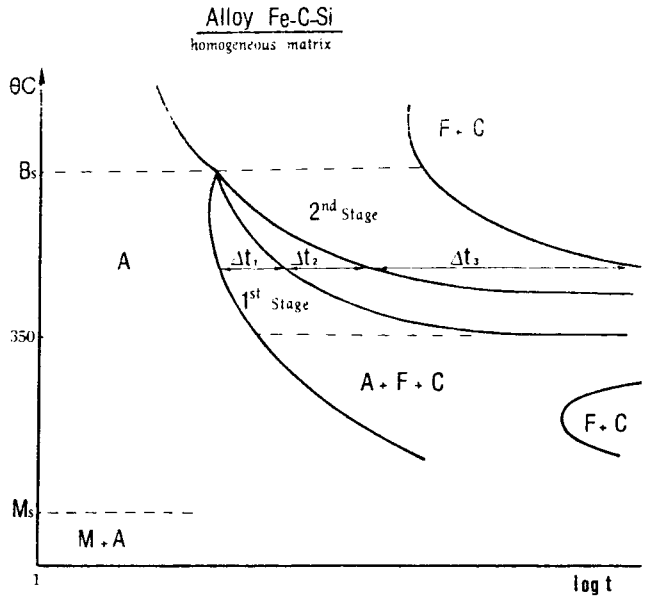

$350 \leqslant \theta \leqslant Bs$	
1st Stage	$\gamma \rightarrow (\alpha) + (\gamma)$
2nd Stage	$(\gamma) \rightarrow \alpha$ + silicocarbide
	$(\alpha) \rightarrow \alpha$ + silicocarbide
$\Delta t_i = f(\%C, \%Si, \theta)$	

Fig. 12—Schematic representation of the two stages of the bainitic reaction ($350 < \theta < Bs$) of a Fe-C-Si steel.

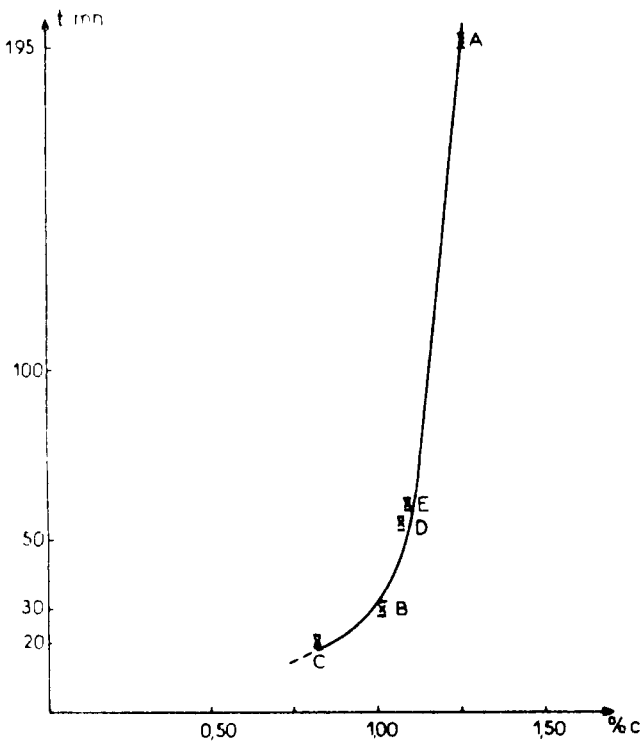

Fig. 13—Influence of carbon content of the parent phase (at constant Si content: 3.7 pct) on the duration of the first stage at 400 °C.

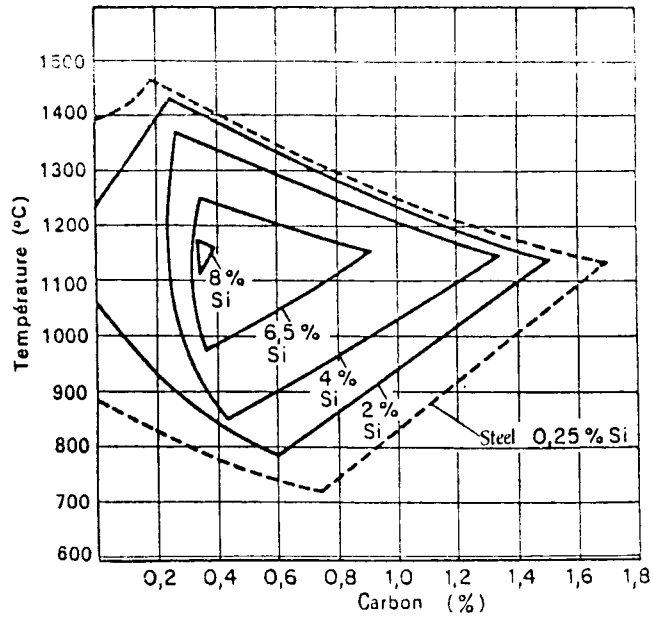

Fig. 14—Influence of silicon content on the stability of the γ phase area.[12]

APPLICATION TO AUSTEMPERED DUCTILE IRON

We have represented in Figure 15(a) the variation in the silicon content inside the matrix between two nodules. This was made on a specimen quenched after an austenitization heat treatment. The composition of the alloy was 3.6 pct C-2.2 pct Si-0.2 pct Mn.

Three zones can be distinguished:

1. In the solidification cell boundary, zone III, the silicon content is the lowest.
2. Near the graphite the silicon content is the highest, zone I.
3. In the major part of the matrix, zone II, the silicon is relatively constant.

The carbon content varies in an inverse manner. In the same way, the manganese is also concentrated at the solidification cell boundary, and the same distribution is observed with phosphorus.

Figure 15(b) shows the influence of segregation on the first stage of the reaction.

1. The Bs and M_s temperatures are different for each zone.
2. The first stage of zone III starts after the first stage of zone II.
3. The kinetics of the reactions differ because the silicon content is lower in zone III than in zone II.
4. Manganese affects this reaction strongly, and its association with silicon can promote a very long first stage.[10,11]
5. Phosphorus does not affect the reaction very much, but it improves the hardenability. Its most important effect is a thermal embrittlement in the range of temperatures from

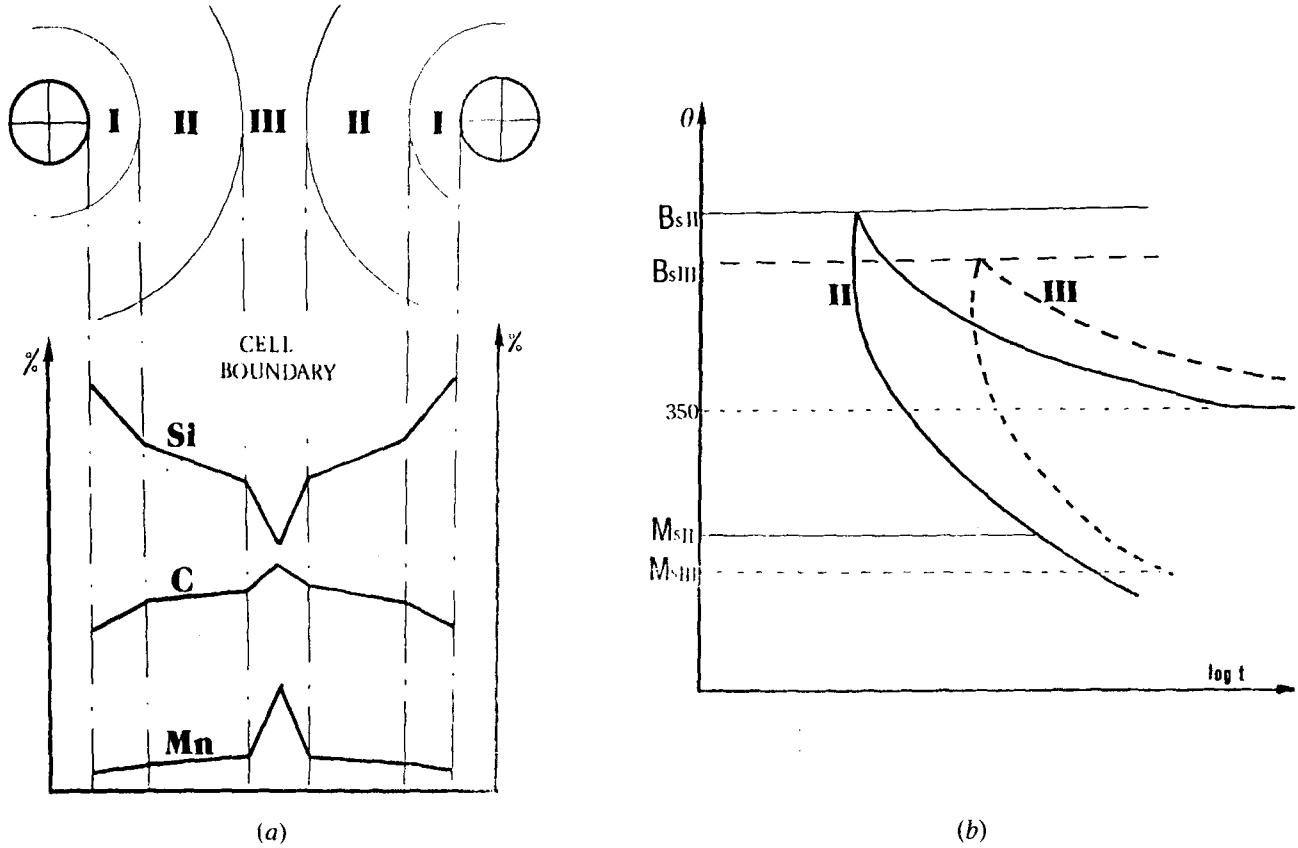

Fig. 15 — (*a*) Representation of the variations in the silicon content and in manganese content inside the matrix of a S.G. cast iron. (*b*) Influence of segregation on the first stage of the bainite reaction (SG cast iron).

350 °C to Bs. However, this embrittlement will occur only after carbide precipitation.

Thus, the second stage of the reaction in upper bainite has a very important role. Figure 16 represents an isothermal heat treatment made at 350 °C. The holding time was previously determined by dilatometric analysis, and in general the reaction seemed to be finished. However, the first stage of zone III is very long and the reaction cannot be finished in this zone.

After a quenching operation, it is very easy to understand that several products will be present in the structure. This has been represented in Figure 17. Because the first stage is not complete in zone III, upon cooling to room temperature this zone will consist of austenite which is not enriched in carbon and martensite. In zone II the first stage is complete. In zone I all kinds of product can be present.

This kind of complex structure is illustrated in Figure 18. A tempering at 200 °C permits one to distinguish easily the black tempered martensite. The virgin martensite is difficult to distinguish from austenite, and this preliminary preparation avoids any confusion between white virgin martensite and the residual austenite. The study of Figure 18 indicates that martensite is present in the cell boundary. The above-described zone III situated at this boundary is an area which is very difficult to transform to bainite.

The amount of segregation is a function of the cell size. Figure 19 shows the structure of the core of the sample before the austempering treatment. The matrice cannot be completely transformed into ferrite, and pearlite remains at

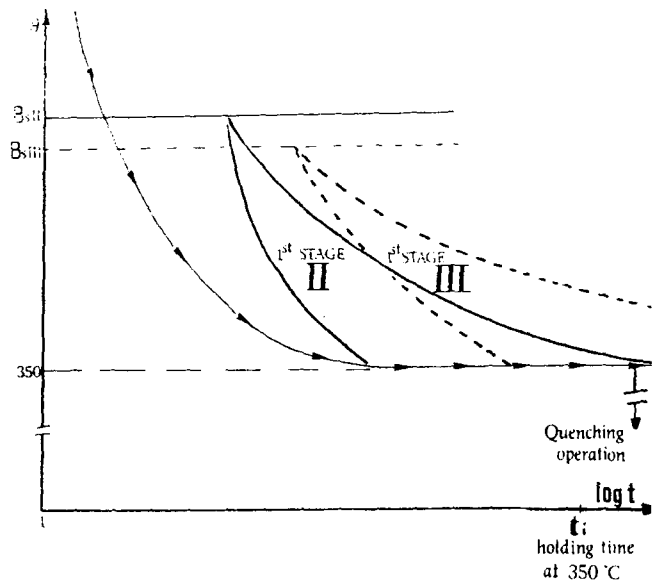

Fig. 16 — Schematic representation of the rate of the first stage reaction in Zones II and III.

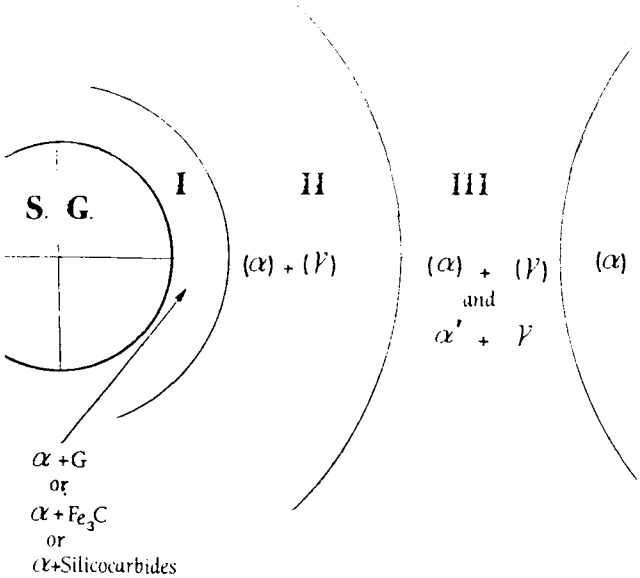

Fig. 17 — Schematic representation of the various microstructures obtained after application of the example described by Fig. 16.

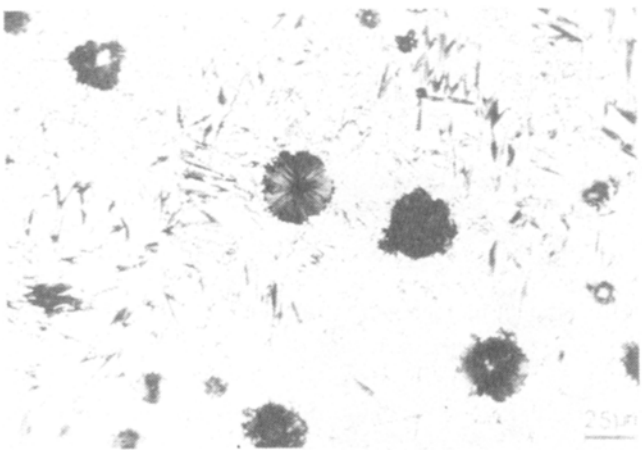

Fig. 18 — OM observation of martensite situated at the solidification cell boundary.

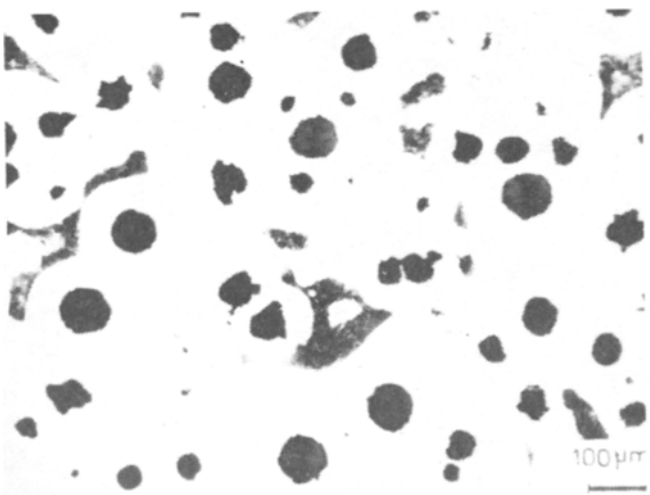

Fig. 19 — OM observation of an initial ferritic matrix at the core of a piece.

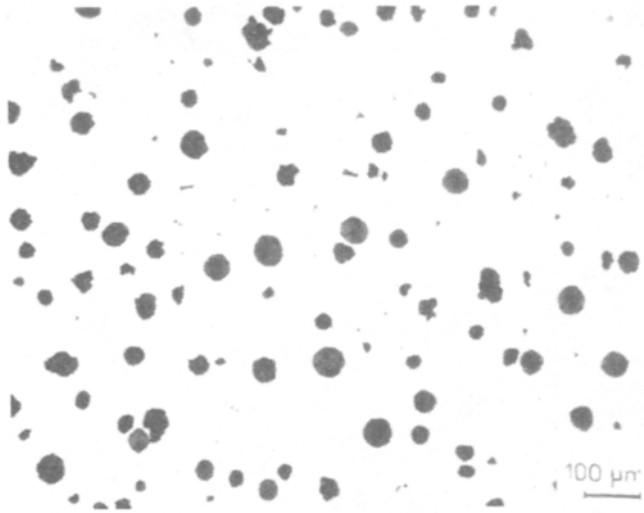

Fig. 20 — OM observation of the ferritic matrix near the surface of the same piece as Fig. 19.

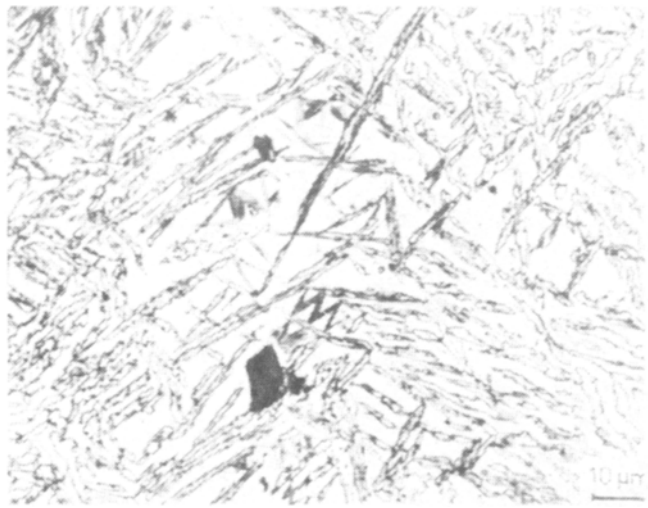

Fig. 21 — OM observation of the matrix at the end of the first stage in a structure containing small cells.

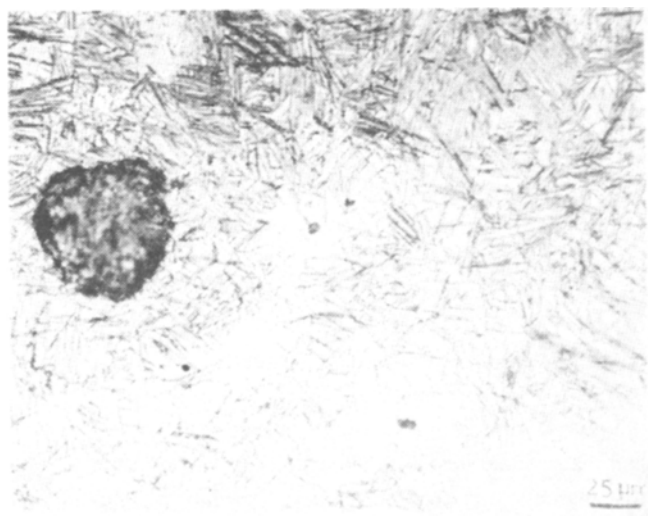

Fig. 22 — Example of the difficulty of separating martensite and austenite located at the cell boundary.

the solidification cell boundaries.[13] In the same sample, the structure of the matrix situated near the surface is completely free of pearlite (Figure 20). Segregation is present, but its level is not sufficient to affect the ferritization reaction. It can be said that the segregation is more important in the core of the pieces because the size of the cells is larger than that observed near the surface.

For the bainite reaction if the initial structure contains small size cells (Figure 21), the segregation is not important, and the separation of different first stage reactions is very slight. The percentage of martensite present in this morphology is very low. If the heat treater does not pay attention, what will happen? Incomplete reaction will occur at the cell boundary producing virgin martensite upon cooling which is difficult to distinguish from austenite (Figure 22). Figure 23 illustrates another example of an incomplete reaction at the cell boundary. The same features can be observed in the case of bainite formed at 300 °C (Figure 24).

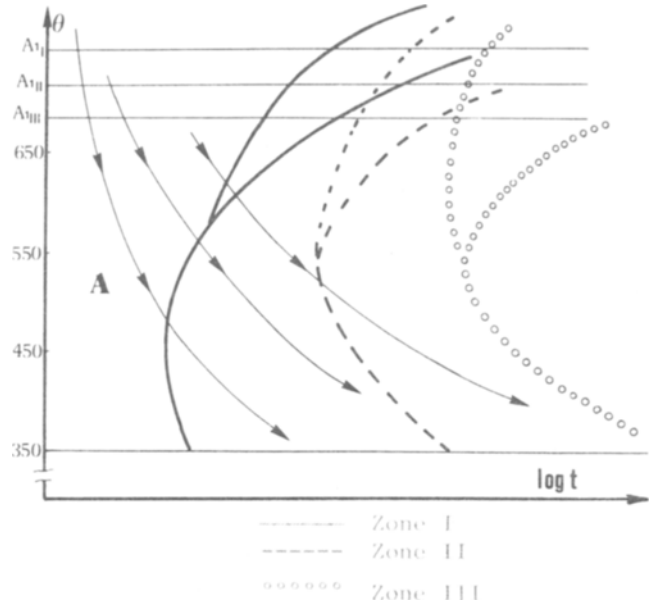

Fig. 25 — Relations between various cooling rates and the local TTT curves of zones I, II, and III.

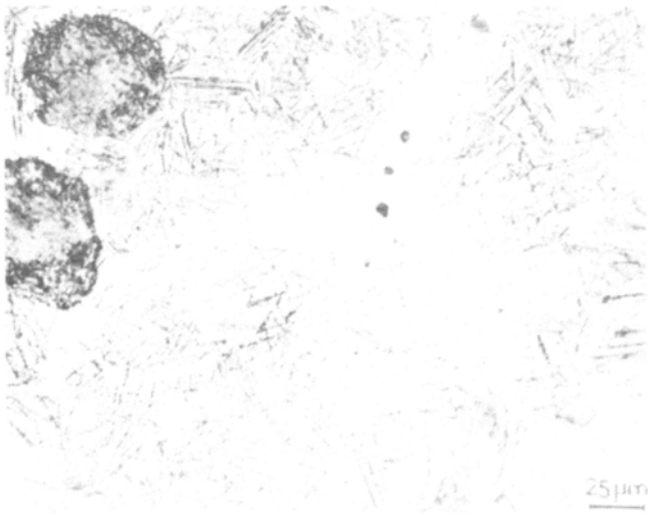

Fig. 23 — OM typical observation of an incomplete first stage reaction (380 °C).

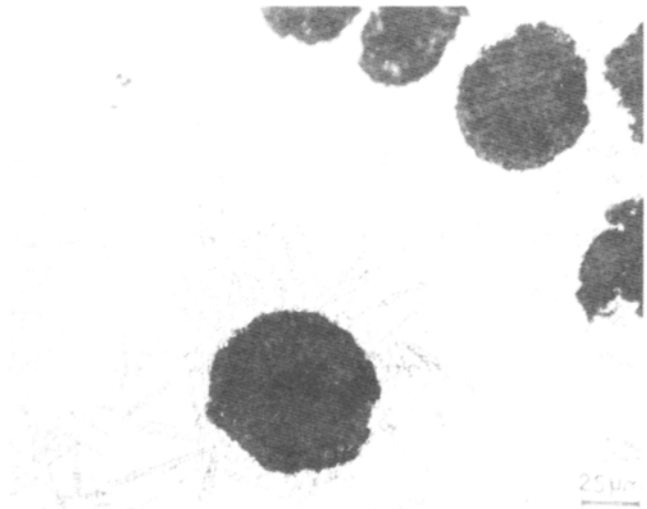

Fig. 26 — Location of the areas of zone I where the bainitic reaction begins.

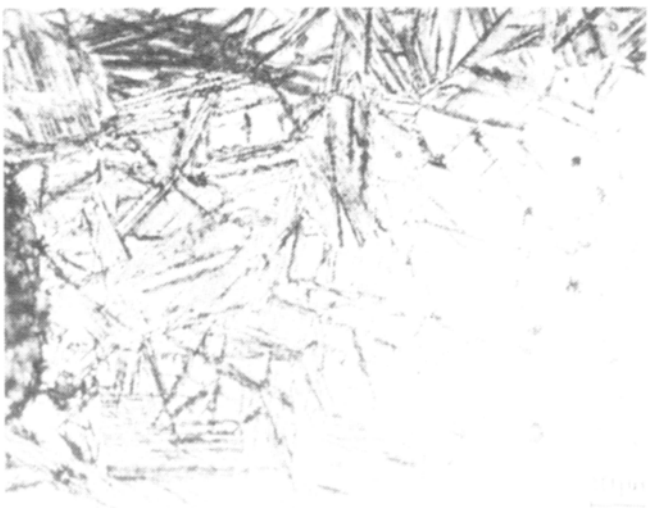

Fig. 24 — Incomplete lower bainitic reaction at the cell boundary (300 °C).

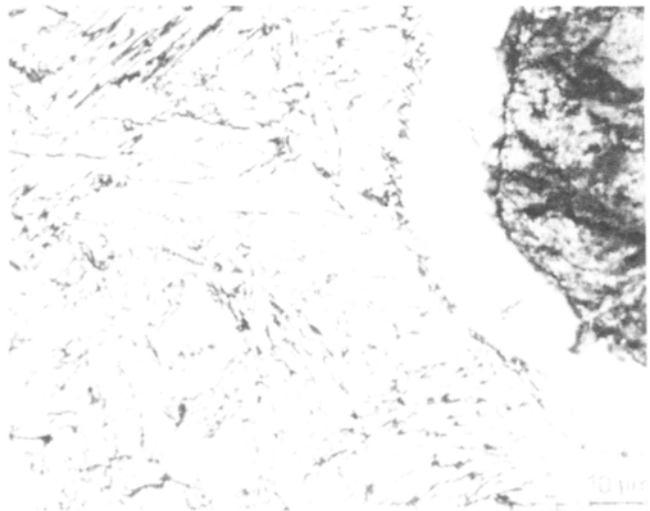

Fig. 27 — Example of formation of a bull's eye near the graphite interface.

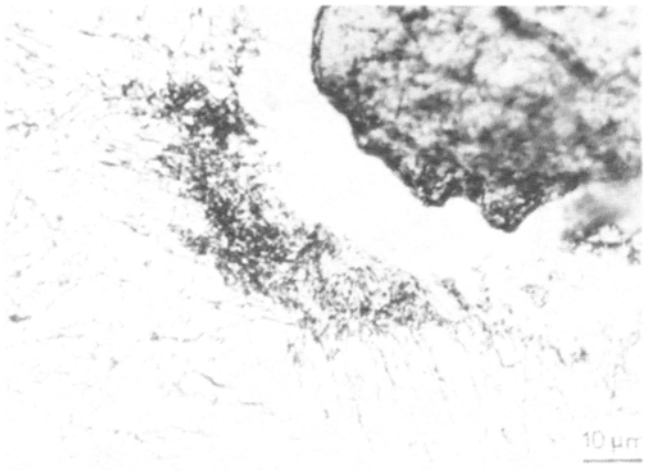

Fig. 28 — Formation of pearlite at the interface between the bull's eye and the bainite.

REACTIONS IN ZONE I

The TTT curve of this zone is situated to the left of the others (Figure 25), and the reactions will always start in this zone. The cooling rate is very important; different kinds of products will be present for different cooling rates. For example, Figure 26 illustrates that the bainite occurs first in zone I. If the cooling rate used to attain the isothermal temperature of heat treatment is too slow, a bull's eye structure appears near the graphite (Figure 27). In some cases (Figure 28) a small amount of pearlite can also be formed between ferrite and bainite. In this example the cooling rate was a little faster than that used in the example shown in Figure 27.

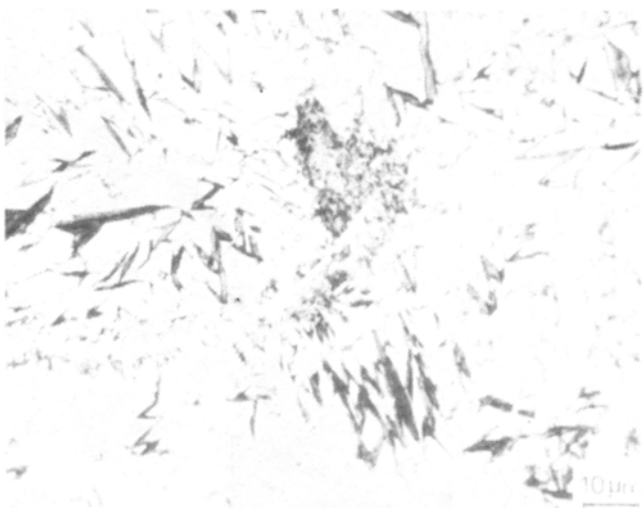

Fig. 29 — Typical aspect of a pro-eutectoid cementite precipitation with formation of pearlite at its interface and martensite. Both of these constituents are situated at the cell boundary.

The structure of the solidification cell boundary at the end of the first stage can also be affected (Figure 29). In this case the initial cooling rate was not fast enough to avoid precipitation of proeutectoid cementite with the removal of carbon in the surrounding austenite. The result is the formation of pearlite. As described before, some martensite is located on each side of this cementite.

SUMMARY

In this paper, different features of the bainitic structures, the origin of the enriched austenite and of the different carbides in austempered ductile iron, have been explained. The influence of the segregation of silicon and manganese on the various kinds of reactions has been discussed.

It is possible to explain why martensite appears at the cell boundary after most of the matrix has transformed to bainite and carbon enriched austenite. It is clear that the most important parameter is the size of the solidification cell because this affects the degree of alloy segregation. For this reason the control of this size is a primary factor.

It is very important to have a better knowledge of the inoculation operation, the inoculation agents, and cooling conditions during solidification. A very high density of nodules will minimize the segregation at cell boundaries and simplify the heat treatment.

REFERENCES

1. C. Bak, J. M. Schissler, J. L. Benard, and M. Degois: *Revue de Fonderie*, May 1981.
2. B. P. J. Sandvik: *Metall. Trans. A*, 1982, vol. 13A, p. 777.
3. H. K. D. H. Bhadeshia: *Acta Metall.*, vol. 28, p. 1103.
4. K. Röhrig: *Giesserei Praxis*, 1983, no. 1/2, p. 1.
5. E. Dorazil, B. Barta, E. Munsterova, L. Stransky, and A. Huvar: *AFS International Cast Metals Journal*, 1982, p. 52.
6. Institut de Recherche de la Sidérurgie, Atlas des Courbes de transformation.
7. J. M. Schissler: Ph.D. Thesis, Nancy, France, 1972.
8. J. M. Oblack and R. F. Hehemann: Transactions and Hardenability in Steels Symposium, 1967, "15".
9. C. Bak: Diplôme d'Etudes Supérieures, Nancy, France, 1975.
10. J. Arnould: Diplôme d'Etudes Supérieures, Nancy, France, 1974.
11. J. M. Schissler, J. Arnould, and G. Métauer: *Revue de Métallurgie*, November 1975, pp. 779–93.
12. E. C. Bain and H. W. Paxton: "Les éléments d'addition dans l'acier", Dunod, Paris, France, 1968.
13. J. M. Schissler, J. Saverna, C. Bak, and R. Bellocci: Volume "Energy Conservation in Industry-Applications and Techniques", Energy R. and D. Programme of the Commission of the European Communities, 1982, pp. 62, 79.